COUPLING MULTIDIMENSIONAL COMPLIANT MODELS FOR CAROTID ARTERY BLOOD FLOW

Santiago Urquiza[1]**, Pablo Blanco**[1]**, Guillermo Lombera**[1]**,**

Marcelo Venere[2] **and Raúl Feijoo**[3]

1. Laboratorio de Bioingeniería, Facultad de Ingeniería, Universidad Nacional de Mar del Plata.
Av. Juan B. Justo 4302, (7600) Mar del Plata, Argentina. TE: 54-(0223)-4816600-Interno 252
e-mail: santiagourquiza@fi.mdp.edu.ar

2. PLADEMA-CNEA, Facultad de Exactas UNCPBA.Pinto 399, (7000) Tandil.
e-mail: venerem@exa.unicen.edu.ar

3. L.N.C.C., Petrópolis, RJ, Brasil.
e-mail: feij@lncc.br

Key words: hemodynamic, fluid-structure interaction, FEM, Finite Element, coupling 3D-1D

Abstract. *A Finite Element implementation of a model of the blood flow through the carotid artery considering fluid–wall interactions is presented. The Navier–Stokes equations are used as the governing equations for the blood flow while an elastic compliant model is implemented for the arterial wall. Also, the A.L.E. formulation is considered within the blood regions taking into account the domain deformations produced by the wall displacements. The former three-dimensional model is coupled with a one-dimensional one for the entire arterial tree in order to appropriately set inflow and outflow boundary conditions for 3D zones. The reduced 1D model solves the momentum and continuity equations in compliant tubes so as to reproduce the propagation of the pressure pulse in the arterial network. At the proximal entrance a volumetric flow rate is imposed as the inlet boundary condition to model the systolic work of the heart. The peripheral arterioles beds are simulated with the well known lumped windkessel model. The 3D Navier-Stokes problem is discretized with P1 Bubble-P1 tetrahedral elements using a standard geometry of the Carotid bifurcation. The obtained results adequately reproduce the general flow patterns reported in the literature. It is worthwhile to note that this kind of models may provide useful information for early detection, prevention and diagnosis of related arterial diseases.*

1 INTRODUCTION

Arterial vessel trees perform the vital task of efficiently supplying blood to all organs and tissues of the body carrying nutrients and removing catabolic products. Hemodynamic simulation studies have been frequently used to gain a better understanding of functional, diagnostic and therapeutic aspects of the blood flow. These simulations employed compartmental representations or branching tube models of arterial trees as their geometrical substrate[1],[24][27], as well as localized three-dimensional models have been often implemented to study arterial flow in more fine, detailed aspects[4],[8],[20],[23].

The study of the flow in the carotid artery bifurcation is of great clinical interest with respect to both, the genesis and the diagnostics of atherosclerotic diseases. It is well-known that the flow separation zone of the carotid sinus has the propensity to develop atherosclerotic plaques. In this sense, the local haemodynamic structure is intimately related to atherogenesis onset and progress [2]. Consequently, a more deep understanding and better descriptions of the flow structure in that region would be of the greatest importance to the early detection of stenoses. Low shear stress regions are associated with the development of stenotics plaques. Despite the importance of chemical and physiological factors, the localized atherosclerotic lesions must be related to the local flow conditions as the other factors may be considered in a well mixed condition, i.e., uniformly distributed along the vessels.

Several local three-dimensional (3D) in-vitro and computational flow models have been implemented, revealing the complex flow structure in the sinus district. Bharadvaj et. al.[28][29], defined a standard geometry of the carotid bifurcation (an average over 57 actual geometries from different subjects) and conducted stationary studies of the internal carotid blood flow. They found a region of low velocities near the non-dividing wall that extend with increasing Reynolds number, correspondingly, the opposite region showed large axial velocities and shear stresses, results that were confirmed by Rindt et. al[4], using experimental and computational stationary models. Ku and Giddens[5][7] observed a similar process in 3D models during the accelerating period of the diastole and the existence of velocities disturbances during the decelerating phase and at the onset of the diastole. Some similar experiments have been conducted in compliant models[14].

To conduct focused numerical and in vitro realistic experiments of such a district as the carotid bifurcation, special attention must be paid to the boundary conditions applied to the model. As the pressure differences between inlet and outlet boundaries are only a small percentage of the systolic-diastolic pulse amplitude, this impose the problem of accurately determine the pressure, a condition that is often impossible to reach in practice. In this way, small errors in the imposed pressure could lead to great departure of the velocities from the real values. Conversely, if the flow is imposed as boundary conditions, negligible variations on these values could conduct to exaggerated low o high pressures in the analyzed segment. Accurate enough measures of those variables are very difficult or very costly to obtain simultaneously at the inflow and outflow regions for the entire cardiac period, even more in a noninvasive manner. This in turn, leads to implement models of the whole arterial tree in order to avoid artificial boundaries in the vicinity of the analyzed zone. Three-dimensional

233

models of the whole arterial tree are, at the present times, unrealizable due to the computational costs well exceed capabilities of modern computers and/or it is a very compromised task to obtain and manage all the information (geometric and physiologic) necessary to construct such detailed models. Consequently, it is an interesting idea to model localized zones with great detail as 3D districts coupled with a 1D model of the rest of the arterial tree with less parameter involved and decreased complexity, that serves as boundary conditions provider to the former.

Recently, the coupling and integration of models with different dimensionality have been analyzed by Quarteroni, et. al. [16][21] linking together lumped models with 3D models of the arterial tree. This task is very cumbersome since this problem involve deformable domains (compliant arteries walls), as well as, other nonlinearities in the governing equations such as convective terms and fluid structure interactions besides regions of diverse dimensionality and the coupling conditions between them. The authors of the present work has proposed an alternative approach to coupling models of non-matching dimensionality and used them to implement a model of stenoses in the common carotid[12]. Here we implement a 3D finite element model of the carotid bifurcation on a standard geometry as proposed in [28][29] coupled with a 1D model of the rest of the arterial tree. Flow patterns for an entire cardiac period are obtained and analyzed in order to gain insight in the complexity of the unsteady flow in that region and also to evaluate the computational requirements for an accurate representation of the phenomena.

2   THE MODEL

2.1 Governing equations

A complete model of the arterial tree was developed with a three-dimensional model of the carotid bifurcation embedded in a reduced 1D Navier-Stokes equations considering compliant arterial walls for the rest of the arterial tree. The governing equations for the 1D portion of the model result in the following set of nonlinear hyperbolic equations:

$$\frac{\partial Q}{\partial t}+\frac{\partial}{\partial x}(a\,\frac{Q^2}{A})=-\frac{A}{r}\frac{\partial P}{\partial x}-\frac{p.D}{r}.t_o \tag{1}$$

$$\frac{\partial A}{\partial t}+\frac{\partial Q}{\partial x}=0 \tag{2}$$

with

$$a=\frac{A\int u^2 dA}{Q^2}\quad ;\quad \tau_o=f_r.\frac{\rho\,\tilde{u}.|\tilde{u}|}{8}\quad ;\quad Q=\tilde{u}.A\; ; \tag{3}$$

where A is the artery cross sectional area, u the axial velocity ($\tilde{u}$ the corresponding mean value); x the axial coordinate, P the mean pressure, ρ the blood density, t_o the viscous shear

stress acting on the arterial wall with f_r a Darcy friction factor (in this work a fully developed parabolic velocity profile is considered) and α is a correction factor for the axial momentum.

A closure equation is implemented relating the pressure to the cross sectional area:

$$P = P_o + E h_o/R_o \left[\sqrt{\frac{A}{A_o}} - 1 \right] \qquad (4)$$

A linear relationship between P and R is considered, being R de radius, E an effective Young modulus, h the thickness of the arterial wall and the subscript "o" denotes quantities evaluated at the reference pressure P_o.

The former system of partial differential equations is discretized using a Galerkin Least-Squares method for the normal equations of the hyperbolic system[12].

The local 3D fluid dynamics was described using the 3D time-dependent Navier-Stokes equations for incompressible Newtonian fluids where an A.L.E. method was implemented in order to take into account deformability of the domain as the arterial walls were considered as compliant tubes:

$$r\frac{\partial \mathbf{u}}{\partial t} + r(\mathbf{u} - \mathbf{v}) \cdot \tilde{\mathbf{N}}\mathbf{u} - m\tilde{\mathbf{N}}^2\mathbf{u} + \tilde{\mathbf{N}} p = \mathbf{f}$$
$$div\ \mathbf{u} = 0 \qquad (5)$$

$$\tilde{\mathbf{N}}^2 \Delta \mathbf{x} = 0 \qquad (6)$$

where $\mathbf{u}$ is the fluid velocity, $\mathbf{v}$ is the moving reference frame velocity consistent with the A.L.E. formulation, p is the pressure, $\Delta \mathbf{x}$ is the displacement vector of the moving domain from its reference configuration, $\mathbf{f}$ are the volume distributed forces, ρ and μ stand for the constant fluid density and the dynamic viscosity, respectively. This set of equations must be supplied with appropriate boundary conditions and closure equations. As the domain moves with the arterial wall, a relationship for representing the arterial wall compatible with the 1D model must be provided. The simplest model that accomplishes these requirements is that of independent rings. This was implemented concordantly with the following equations for points on the surface $\partial \Omega_w$ that represents the arterial wall:

$$P - P_o = \frac{E h}{R_o^2} \boldsymbol{d}$$
$$\Delta \mathbf{x} = \boldsymbol{d}\, \boldsymbol{n}\ ;\ \mathbf{u} = \frac{d\Delta \mathbf{x}}{dt} \qquad (7)$$

where δ is the displacement of the arterial wall in the normal direction of the surface ($\boldsymbol{n}$ is the unit normal to the surface). The first of equations (7) is analogous to that of the 1D model given in eq (4).

Another group of equations must be considered to appropriately set the coupling between the 1D and the 3D models at the interface surfaces. Continuity of mass, momentum and

tractions must be imposed. For the Reynolds numbers prevailing at the carotid artery, continuity on tractions may be replaced by continuity on pressure. Consequently, continuity of blood flow is enforced at the interfaces between 1D and 3D zones jointly with weak continuity of pressures as described in [12]. We note here that, momentum continuity is implied in the correct choice of the parameter α in equation (3) that must be evaluated nonlinearly from the results on the 3D model. Here we have used $\alpha = 1$ constant, and consequently the former requirement is not completely fulfilled But it must be noted that relaxing this condition don't produce significant spurious reflections in the case of long wavelengths, as is in the present case. This is a very simple and efficient alternative to coupling zones with diverse dimensionality compared with those proposed in [17] and lead to a solution scheme where the 1D model is solved together with the 3D zones avoiding costly subdomain decomposition, observe that the unknowns corresponding to the 1D are a few percentage of the total.

2.2 Numerical approach

For the numerical solution of the 3D flow problem the finite element method was applied: the approximation makes use of P1-P1 bubble tetrahedral elements with linear enriched interpolation functions for the velocity vector field and linear pressure[15].
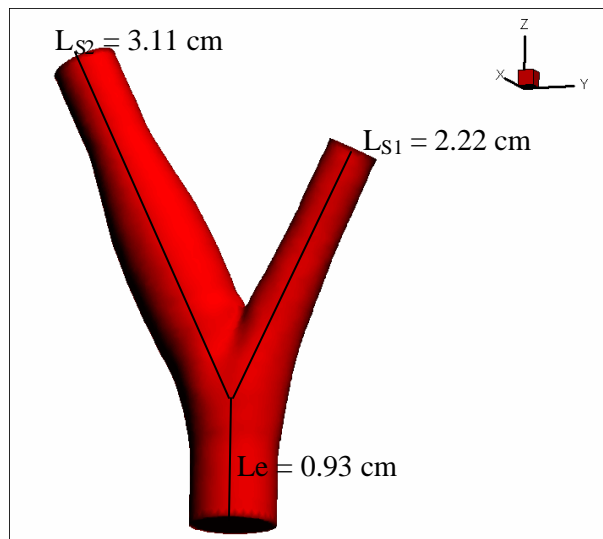

Figure 1: *3D carotid bifurcation geometry model*

The equations are solved using the finite element SUPG method with implicit Euler backward differences for the time derivatives and Picard iteration for the non-linear convection terms. The solution of the time-dependent 3D Navier-Stokes equations is performed in two sub-steps: in the first one, the bubble degrees of freedom are eliminated by direct substitution, and in the second one, those unknowns are updated as necessary for the

evaluation of the second member of the set of equations at the following time step. The deformation of the domain is accounted through a Laplace equation for the displacement of the mesh –again, tetrahedral linear elements are used- where the boundary displacements at the arterial wall are given by the first of eq. (7). Flow velocity patterns were calculated for an anatomically inspired carotid artery bifurcation model[28] [29] as shown in Figure 1, the 3D mesh exposed in Figure 2 has 14159 nodes and 71732 tetrahedral elements.
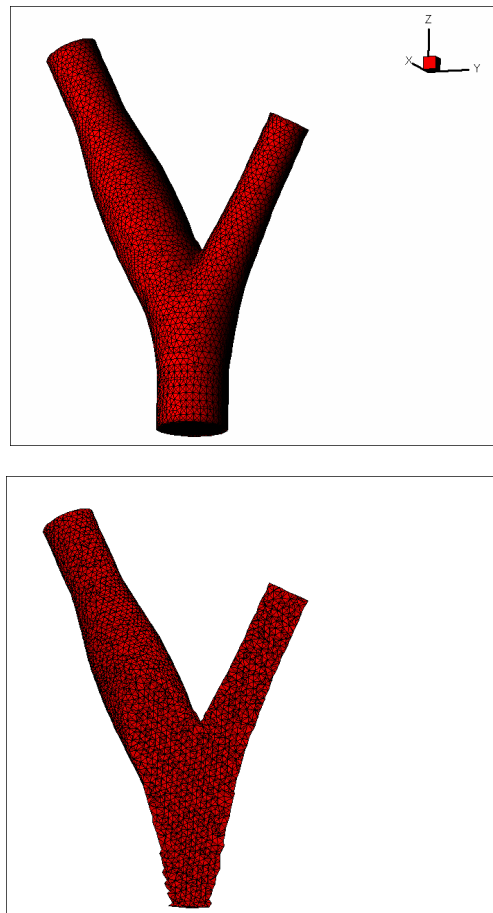
Figure 2: 3D *FEM mesh –tetrahedral elements-*

The one-dimensional model was described in Urquiza[12] discretized with a mesh displaying 686 nodes with three degrees of freedom (A, P, Q) per node and 642 elements. The inlet boundary condition describing the heart input flow was obtained from [22] and has a period T=0.8sec. The model is complemented with lumped "Windkessel" representations of the peripheral beds. The geometry and other parameters involved are shown in Figure 3 and

237

also in tables 1-2, see reference [12] for additional details. Finally, the selected values for ρ and μ were 1.04 gr/cm^3 and 0.04 Poise in that order.

Table 1: Windkessel terminals

	Name	R1	R2	C
		dinas.seg/cm²/ml		ml.cm²/dinas
1	Coronary	10.00E3	41.00E3	.7900E-5
2	Intercostals	2.78E3	11.12E3	.1638E-4
3	Gastric, Hepatic & Esplenic	2.54E3	10.17E3	.2967E-3
4	Renal (two)	1.26E3	5.04E3	.1235E-3
5	Superior mesenteric	1.92E3	7.68E3	.1726E-3
6	Inferior mesenteric	16.62E3	66.46E3	.7400E-4
7	Internal iliac	17.04E3	68.17E3	.6750E-4
8	Deep femoral	11.60E3	46.39E3	.5030E-5
9	Anterior tibial	56.15E3	224.61E3	.4170E-5
10	Posterior tibial	9.54E3	38.16E3	.3900E-5
11	Vertebral	16.65E3	66.60E3	.9880E-4
12	Interosseous	211.74E3	846.96E3	.3107E-6
13	Ulnar	10.56E3	42.24E3	.3520E-5
14	Radial	10.56E3	42.24E3	.3520E-5
15	Carotid	6.31E3	25.55E3	.1330E-5

Table 2: Geometric and rheologic values of arterial segments

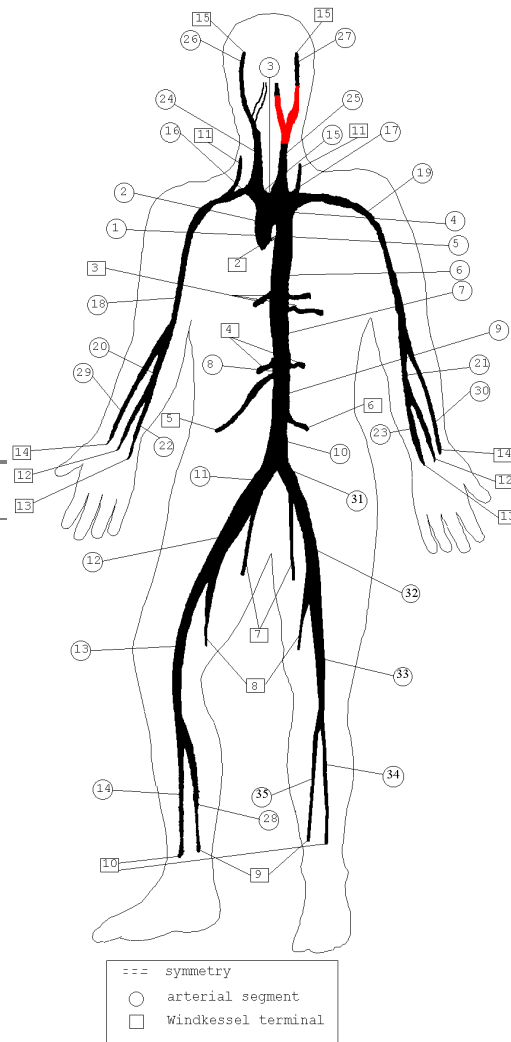|	name	Length (cm)	Proximal radius (cm)	Distal radius (cm)	$E \times h$ (dinas/cm)
1	Ascending aorta A	1.0	1.46	1.46	741500
2	Ascending aorta B	3.0	1.45	1.45	741500
3	Aortic arch A	2.0	1.12	1.12	741500
4	Aortic arch B	3.9	1.07	1.07	576200
5	Thoracic aorta A	5.2	1.0	1.0	545640
6	Thoracic aorta B	10.4	0.675	0.675	394000
7	Abdominal aorta A	5.3	0.61	0.61	370500
8	Abdominal aorta B&C	2.0	0.6	0.6	348000
9	Abdominal aorta D	10.6	0.58	0.58	352400
10	Abdominal aorta E	1.0	0.52	0.52	252500
11,31	Common iliac	5.8	0.37	0.37	368150
12,32	External iliac	14.4	0.32	0.32	148700
13,33	Femoral	44.3	0.26	0.26	230900
14,34	Posterior tibial	33.1	0.25	0.25	667500
15	Innominate	3.4	0.62	0.62	377000
16,17	Subclavian A	3.4	0.423	0.423	288700
18,19	Subclavian B	42.2	0.403	0.403	1170000
20,21	Ulnar A	6.7	0.215	0.215	679100
22,23	Ulnar B	17.1	0.203	0.203	717664
24,25	Carotid	20.8	0.37	0.37	264000
26,27	External carotid	17.7	0.177	0.177	259000
28,35	Anterior tibial	34.3	0.13	0.13	513145
29,30	Radial	23.5	0.174	0.174	682580

Figure 3: *Arterial tree scheme*

The whole model was computationally implemented in a numerical framework[11] that allows to easily integrate different kinds of elements as "plug and play" without modifying the main program, i.e., the programmer only must to provide the elemental matrices and to organize the input in such a way that all run together. The linear equations are solved by a preconditioned (LU incomplete decomposition from SparseKit[10]) Conjugate Gradient Squared method[9] although similar performance may be obtained with BCG Stabilized[10]. The cardiac period (T=0.8 sec.) was divide into two equal intervals of 0.4 sec. For the systolic subperiod a time step of 2.5E-3 sec was used, and for the diastolic one was selected a time step of 5E-3 sec. In this way a very efficient and cost effective solver of the problem was implemented making possible to obtain the results in a one day run on a PC platform.

3   RESULTS

Here we present some illustrative plots at selected times. In general, the flow has a very complex and unsteady structure showing an early back flow due to the inversion of the pressure gradient at the peak of the systole (Figure 5).

A considerable deformation of the artery volume can be observed in Figure 4 where volume differences during diastole (red shaded) and systole (black wire frame) are displayed.
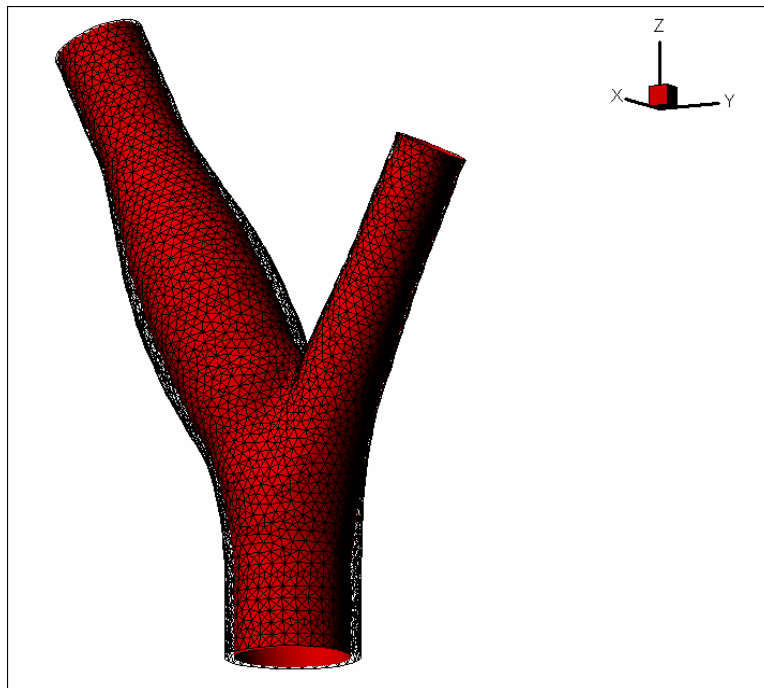

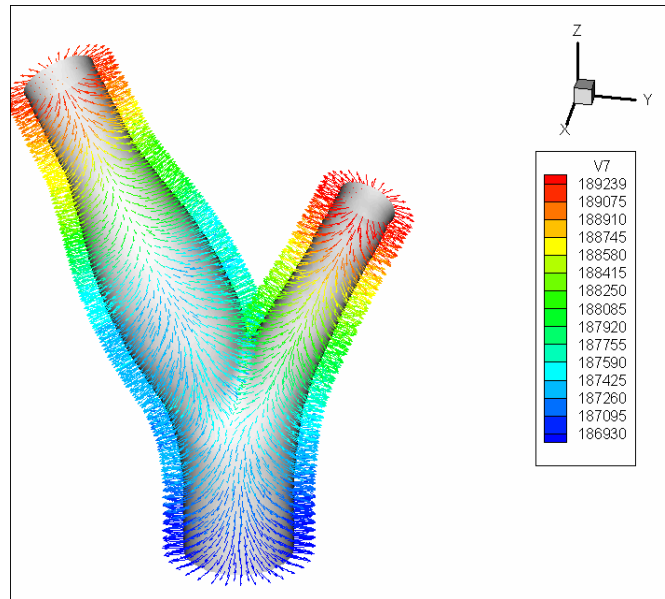Figure 4: *Volume differ ence between systole and diastole*

Figure 5: *Normal Stress during systole at t = 5.0E-2 sec. -Inverse pressure gradient.-*
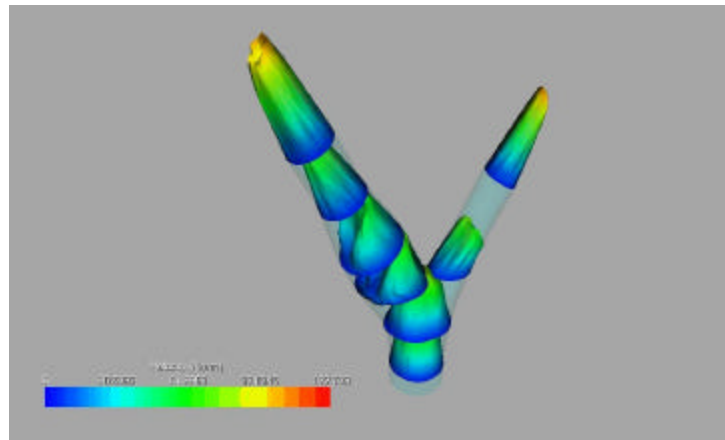

Figure 6: *Velocity during systole*

As can be seen in Figure 6 a zone of low velocities near the non-divider wall of the carotid sinus is observed and contrariwise, a high velocity region is displayed near the divider wall. These results are in well agreement with those obtained experimentally and numerically in references [8][28][29][14]. Detailed inspection of the computational results displays the general characteristics occurring in the carotid sinus, a period with reverse axial flow starts at the peak systole and remains until the beginning of diastole. This is illustrated for the Vz component of the velocity vector during the decreasing phase of the systole as shown in

Figure 7. Also in that figure can be observed a typical Womersley flow at the entrance, where the flow reversal occurs at the outer ring while at the center the velocity remains positive.
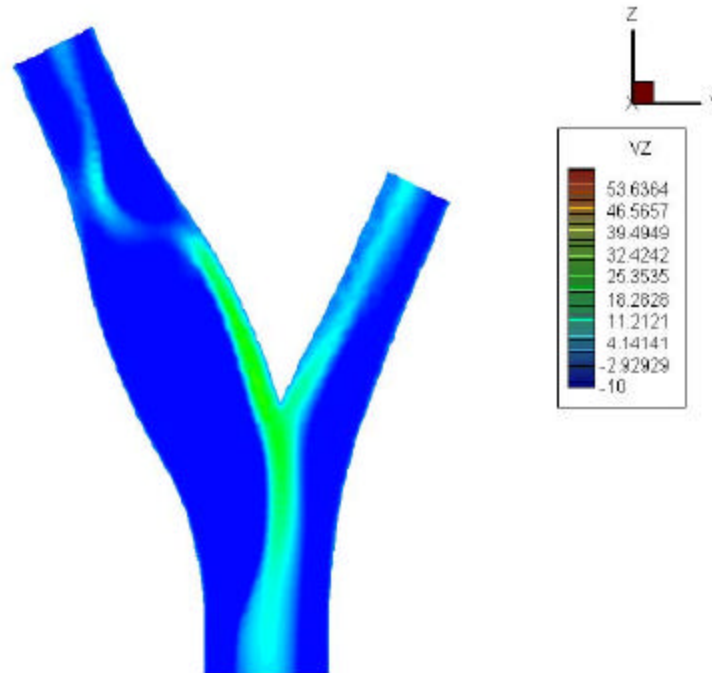

Figure 7: *Back flow during late systole*

Also the outflow velocity profile for the internal and external carotid were integrated over the duration of the cardiac cycle and compared with that for the inflow condition, resulting in conservation of mass higher than the 99.5%.

4 CONCLUSIONS

A computational model that face the problem of simulating compliant 3D arterial districts coupled with a 1D model of the rest of the arterial tree was presented. The resulting scheme has shown excellent capabilities to deal with considerable domain deformations while preserving the computational efficiency. Calculations of the flow field for the carotid artery are in general good agreement with those reported previously in the literature for both experimental and numerical cases. This class of models can contribute to take into account more realistic boundary conditions when studying three dimensional zones of the arterial tree and also, being very helpful to understand the flow patterns that influence the start and development of the atherosclerotic disease.

5 REFERENCES

[1] P. Bruinsma, T. Arts, J. Dankelman, J.A.E. Spaan, Model of the coronary circulation based on pressure dependence of coronary resistance and compliance, Basic Res. Cardiol. 83 (1988) 510-524.

[2] Caro C.G., Fitzgerald J.M. Schroter R.C., Atheroma and arterial wall observations, correlation and proposal of a shear dependent mass transfer mechanism for atherogenesis, Proc. R. Soc. London, B177, 109-159, 1971.

[3] Gijsen F.J.H. et. al. Analysis of the axial flow fields in stenosed carotid artery bifurcation models:LDA experiments, J. Biomechanics, V29, Nº11, pp.1483-1489, 1996.

[4] Rindt, C.C.M., Steenhoven, A.A., van Janssen, J.D., Reneman, R.S., Segal, A., 1990. A numerical analysis of steady flow in a three-dimensional model of the carotid artery bifurcation. Journal of Biomechanics 23, 461-473.

[5] Ku, D.N., Giddens, D.P., 1985. Hemodynamics of the normal carotid bifurcation. Ultrasound in Medicine and Biology 11 (1), 13}26.

[6] Ku, D.N., Giddens, D.P., 1987. Laser Doppler anemometer measurements of pulsatile flow in a model carotid bifurcation. Journal of Biomechanics 20, 407-421.

[7] Ku, D.N., Giddens, D.P., Zarins, C.K., Glagov, S., 1985. Pulsatile flow and atherosclerosis in the human carotid bifurcation. Arteriosclerosis 5 (3), 293-302.

[8] Botnar Rene H, Rappitsch G., Scheidegger M.B., Liepsch D., Perktold K., Boesiger P., Hemodynamics in the carotid artery bifurcation: a comparison between numerical simulations and in vitro MRI measurements, Journal of Biomechanics 33, pp.137-144, 2000.

[9] Sonneveld P. et al, "Multigrid and Conjugate Gradient Methods as Convergence Acceleration Techniques", in "Multigrid Methods for Integral and Differential Equations", Clarendon Press, Oxford, 1985.

[10] Saad Yuocef, SPARSEKIT: a basic tool kit for sparse matrix computation, version2, University of Illinois, http://www-users.cs.umn.edu/~saad/software/SPARSKIT/sparskit.html, 1994.

[11] Urquiza S.A., Venere M. J. "An Application Framework Architecture For Fem And Other Related Solvers", pp. 3099-3109, ISSN 1666-6070, MECANICA COMPUTACIONAL Vol.XXI, S. Idelsohn, V. Sonzogni, A. Cardona Eds., CERIDE, Sta Fe, 2002.

[12] Urquiza S. ,Reutemann A., Vénere M., Feijoo R., "Acoplamiento de Modelos Unidimensionales y Multidimensionales para la Resolución de Problemas Hemodinámicos", ENIEF2001, XII Congress on Numerical Methods and their Applications, October 31 – November 2, 2001, Córdoba – Argentina

[13] Giddens D.P. Zarins C. K. Galvov S. The role of Fluid Mechanics in the Localization and Detection of Atherosclerosis, J. Biomemch. Engng, V115,pp. 588-594, 1993.

[14] Anayiotos A.S., Jones S.A., Giddens, Glagov S. Zarins C.K., Shear Stress at a Compliant Model of the Human Carotid Bifurcation, J. Biomech. Engng, V117, pp. 98-106, 1994.

[15] Pironneau O., "Finite-element methods for fluids", Wiley,New York, 1989.

[16] A. Quarteroni, Modeling the cardiovascular system: a mathematical challenge, Mathematics Unlimited - 2001 and Beyond, B. Engquist and W. Schmid Eds, 961-972, Springer-Verlag, 2001.

[17] Formaggia L.,Gerbeau J.F., Nobile F., Quarteroni A., On the Coupling of 3D and 1D Navier-Stokes Equations for Flow Problems in Compliant Vessels, Comp. Meth.App. Mech & Eng., to appear,2000.

[18] L. Formaggia, F.Nobile, J.-F. Gerbeau, A. Quarteroni, Numerical Treatment of Defective Boundary Conditions for the NavierStokes Equations, EPFL-DMA Analyse et Analyse Numerique Report n.20, 2000.

[19] R, Pietrabissa, A. Quarteroni, G. Dubini, A.Veneziani, F. Migliavacca, S. Ragni, From the Global Cardiovascular Hemodynamics down to the Local Blood Motion: Preliminary Applications of a Multiscale Approach, ECCOMAS 2000, E. Oñate et el. (Eds.), Barcelona, 2000.

[20] Alfio Quarteroni, Massimiliano Tuveri and Alessandro Veneziani, Computational Vascular Fluid Dynamics: Problems, Models and Methods, Computing and Visualisation in Science, 2000, vol 2, 163-197.

[21] L.Formaggia. F. Nobile, A. Quarteroni, A. Veneziani, Multiscale Modelling of the Circulatory System: a Preliminary Analysis, Comput. Visual. Sci., 1999, vol 2 issue 2/3, pag. 75-83.

[22] Stettler J.C., Niederer P., Anliker M., "Theoretical Analysis of arterial hemodynamics including the influence of bifurcations", Annals of Biomedical Engineering, 1980.

[23] Perktold K., G. Rappitsch, Computer simulation of local blood flow and vessel mechanics in a compliant carotid artery bifurcation model, J. Biomech. V28 Nº7, pp 845-856, 1995.

[24] Snyder MF, Rideout VC, Hillestad RJ. Computer Modeling of the Human Systemic Arterial Tree. J. Biomechanics Engineering, 1968, 1: 341-353.

[25] Avolio AP. Multi-branched model of the human arterial system. Med. Biol. Eng. Comp. 1980, 18: 709-718.

[26] Stergiopulos N, Young DF, Rogge TR, Computer simulation of arterial flow whit applications to arterial and aortic stenoses. J. of Biomechan. 1992, 25: 1477-1488.

[27] Schaaf, BW, Abbrecht PH. Digital Computer Simulation of Human Systemic Arterial Pulse Wave Transmission: A Nonlinear Model. J. Biomechanics Engineering. 1972, 5: 345-364.

[28] Bharadvaj B,K., Mabon R.F.and Giddens D.P.Steady flow in a model of the human carotid bifurcation-I. Flow Visualization, J. Biomechanics, V15,349-362,1982.

[29] Bharadvaj B,K., Mabon R.F.and Giddens D.P.Steady flow in a model of the human carotid bifurcation-I. Laser-Doppler anemometer measurements, J. Biomechanics, V15,363-378,1982.